Pharmaceutical Research, Vol. 25, No. 6, June 2008 (© 2008)
DOI: 10.1007/s11095-008-9531-5

Research Paper

Eupatilin Protects Gastric Epithelial Cells from Oxidative Damage and Down-Regulates Genes Responsible for the Cellular Oxidative Stress

Eun-Ju Choi,[1] Hyun-Mee Oh,[1] Bo-Ra Na,[1,2] T. P. Ramesh,[1] Hyun-Ju Lee,[1] Chang-Soo Choi,[3] Suck-Chei Choi,[3] Tae-Young Oh,[4] Suck-Jun Choi,[5] Jeong-Ryong Chae,[6] Sang-Wook Kim,[7] and Chang-Duk Jun[1,2,8]

Received August 14, 2007; accepted January 2, 2008; published online February 26, 2008

Purpose. The formulated ethanol extract (DA-9601) of *Artemisia asiatica* has pronounced anti-inflammatory activities and exhibits cytoprotective effects against gastrointestinal damage. Here we investigated whether eupatilin, a major component of DA-9601, has a property of antioxidant activity and protects gastric epithelial cells from H_2O_2-induced damage.
Methods. The protective effect of eupatilin against H_2O_2-induced damages was studied in gastric epithelial AGS cells by measuring wound healing, cell proliferation, and cell viability. Global gene expression profiling was obtained by high-density microarray.
Results. Hydrogen peroxide significantly delayed epithelial migration in wounded area. In contrast, eupatilin prevented the reduction of epithelial migration induced by H_2O_2. Eupatilin also ameliorated H_2O_2-induced actin disruption in AGS cells. Interestingly, treatment with eupatilin dramatically inhibited $FeSO_4$-induced ROS production in a dose-dependent manner. In addition, eupatilin protected cells from $FeSO_4$-induced F-actin disruption. With high-density microarray, we identified dozens of genes whose expressions were up-regulated in H_2O_2-treated cells. We found that eupatilin reduces the expression of such oxidative-responsible genes as HO-1, PLAUR and TNFRSF10A in H_2O_2-treated cells.
Conclusion. These results suggest that eupatilin acts as a novel antioxidant and may play an important role in DA-9601-mediated effective repair of the gastric mucosa.

KEY WORDS: anti-oxidant; eupatilin; microarray; reactive oxygen species; wound healing.

INTRODUCTION

Extracts of *Artemisia asiatica* has been traditionally used for the treatment of such diseases as inflammation, cancer and microbial infection. In fact, a novel antipeptic formulation prepared from the ethanol extracts of *A. asiatica*, namely, DA-9601 (Stillen™), has been reported to possess anti-oxidative and anti-inflammatory activities on experimentally induced gastrointestinal damage as well as hepatic and pancreatic lesions (1–4). DA-9601 is now on the market in South Korea and will be on sale in other Asian countries in the near future. However, despite of those studies in animals and in human subjects, the underlying mechanisms of DA-9601-mediated protection are largely unidentified.

Eupatilin is one of the pharmacologically active ingredients of DA-9601. However, most studies regarding the function of eupatilin *in vitro* are attributed to the induction of apoptosis in many cell types (5–8). For example, eupatilin inhibited the growth of MCF-10A-*ras* cells by inhibiting the expression of cell cycle regulators such as cyclin D1, cyclin B1, Cdk2 and Cdc2 (8). Eupatilin also induced apoptotic cell death in gastric epithelial AGS cells by elevating the expression of p53 and p21 (6).

It is interesting to be noted that some herbal medicines have been shown to possess a variety of biological activities at nontoxic concentrations in cells or organisms. Flavonoids are well known examples and have various functions including carcinogen inactivation, anti-proliferation, cell cycle arrest, induction of apoptosis and differentiation, inhibition of angiogenesis, anti-oxidation and reversal of multi-drug resistance or a combination of these functions (9). Resveratrol is also another good example. It has been demonstrated that resveratrol induces apoptosis and causes cell cycle arrest in various cell types (10–12). Meanwhile, there are also numerous reports

Eun-Ju Choi and Hyun-Mee Oh contributed equally to this work.

[1] Department of Life Science, GIST, Gwangju, 500-712, Korea.
[2] Cell Dynamics Research Center, BioImaging Research Center, and Research Center for Biomolecular Nanotechnology, GIST, Gwangju, 500-712, Korea.
[3] Digestive Disease Research Institute, Wonkwang University School of Medicine, Iksan, Chonbuk 570-749, Korea.
[4] Research Institute, Dong-A Pharmaceutical Co. Ltd., Yongin, 449-905, Korea.
[5] Department of Leisure Sports, Wonkwang Health Science College, Iksan, Chonbuk 570-749, Korea.
[6] Department of Physical Education, Kunsan National University, Chonbuk, 573-701, Korea.
[7] Department of Internal Medicine, Chonbuk National University College of Medicine, Jeonju, 561-712, Korea.
[8] To whom correspondence should be addressed. (e-mail: cdjun@gist.ac.kr)

ABBREVIATIONS: DHR, dihydrorhodamine 123; DIC, differential interference contrast; MTT, 5-diphenyltetrazolium bromide; PBS, phosphate-buffered saline; ROS, reactive oxygen species.

demonstrating that resveratrol has an anti-oxidative property and protects cells from exogenous pro-oxidative damages (13–16). As eupatilin is a major ingredient of DA-9601, we therefore questioned whether eupatilin has a direct anti-oxidative property and that it may have a function to protect gastric epithelial cells against oxidant-induced damage.

In the present study, we describe the effects of eupatilin on gastric epithelial cell migration and actin cytoskeletal changes induced by H_2O_2 or $FeSO_4$. By utilizing high-density microarray and real-time PCR, we also describe a number of oxidative stress-responsible genes and their down-regulation probably by indirect diminish of H_2O_2 by eupatilin in gastric epithelial AGS cells.

MATERIALS AND METHODS

Reagents and Antibodies

Eupatilin (5) was supplied from Dong-A Pharmaceutical Co. Ltd., (Yongin, South Korea) (2) and dissolved in DMSO for treatment. Unless otherwise indicated, 0.1% of DMSO was used as a vehicle control. The structural formula of eupatilin is shown in Fig. 1. Hydrogen peroxide, dimethyl sulfoxide, phosphate-buffered saline (PBS), TRITC-Phalloidin, propidium iodide (PI) were purchased from Sigma Chemical Co. (St. Louis, MO). Dihydrorhodamine 123 (DHR) was from Molecular Probes, Inc. (Eugene, OR). Cell counting kit-8 (CCK-8) was from Dojindo molecular technologies, Inc (Tokyo, Japan). Ficoll-hypaque was from Amersham Biosciences (Little Chalfont, England).

Cell Culture

Human gastric epithelial AGS cells obtained from the American Type Culture Collection (ATCC) were cultured at 37°C in a 5% CO_2 atmosphere in Ham's F12 medium supplemented with heat-inactivated 10% fetal bovine serum (FBS; Gibco BRL) and appropriate antibiotics. The BALB/c murine macrophage cell line J774A.1 (ATCC TIB-67) was grown in DMEM supplemented with 2 mM glutamine, 100 U/ml penicillin, 100 μg/ml streptomycin, and 10% heat-inactivated fetal bovine serum in 5% CO_2 at 37°C. Human neutrophils were isolated from normal donors by dextran sedimentation followed by centrifugation through a discontinuous Ficoll gradient (Amersham Biosciences, Little Chalfont, England). All the cell lines or primary cells mentioned above were cultured at 37°C in a humidified incubator containing 5% CO_2 and 95% air.

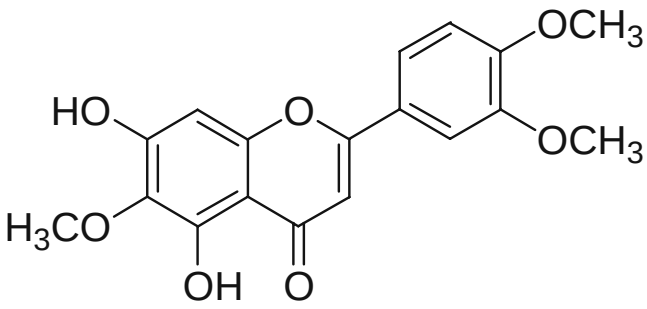

Fig. 1. Structural formula of eupatilin (5,7-dihydroxy-3′,4′,6-trimethoxy-flavone).

Cell Viability Assay

Cellular viability was determined by PI incorporation. Cells were treated with various reagents as indicated in the *Results* section, washed with PBS twice, resuspended in PBS containing 20 μg/ml PI, and then immediately analyzed on a flow cytometer (Becton-Dickinson, Rutherford, NJ). PI-positive cells were counted as dead cells and the remaining cells were designated as viable cells.

In Vitro Wound Assay

In vitro injury was induced in AGS monolayers by creating one to two liner scratches of ±0.3 mm width using a sterile pipette tip, after which detached cells were removed by washing with serum-free media and fresh media containing 10% FBS were added. In some cases, cells were pretreated for 1 h with H_2O_2, eupatilin, or H_2O_2 plus eupatilin, washed with serum-free media, and then further incubated at 37°C in fresh media containing 10% FBS. In case of simultaneous treatment, cells were treated with eupatilin for 1 h before H_2O_2 unless otherwise indicated. Wound closure was followed over 16 h using a differential interference contrast (DIC) equipped with 10X objective in FV1000 confocal laser scanning microscope, and initial and remaining wound areas were determined using FLUOVIEW software ver.1.5 (Olympus corporation, Japan) for calculation of the percentage of wound closure. Cells were also fixed for actin staining as described below "Actin staining of AGS cells"

Cell Proliferation Assay

Cell proliferation was assessed by using the Cell Counting Kit-8 (CCK-8; Dojin, Tokyo, Japan). CCK-8 solution is comprised of WST-8 (2-(2-methoxy-4-nitrophenyl)-3-(4-nitrophenyl)-5-(2,4-disulfophenyl)-2*H*-tetrazolium, monosodium salt) that produces a water-soluble formazan dye upon bioreduction in the presence of an electron carrier (17). WST-8 is reduced by dehydrogenase in cells to give a yellow-colored product (formazan), which is soluble in the tissue culture medium. The amount of the formazan dye generated by the activity of dehydrogenases in cells is directly proportional to the number of living cells. Cultured cells were incubated with CCK-8 solution for 1 h at 37°C, and the absorbance at 450 nm was measured with a spectrophotometer.

Measurement of Reactive Oxygen Species (ROS)

The production of ROS was measured by detecting the fluorescent intensity of oxidant-sensitive probe dihydrorhodamine 123 (DHR, Molecular Probes; 18). Cells (1×10^5/well in 96-well plates) were washed with Lock's buffer and incubated with AM-DHR at 37°C/5% CO_2 for 30 min. The cells were then incubated with eupatilin in the presence or absence of $FeSO_4$. After 30 min of incubation, the kinetics of fluorescent intensity for DHR was recorded using fluorescent plate reader at excitation of 507 nm and emission of 529 nm. The fluorescent readings were digitized using SoftMax Pro.

Actin Staining of AGS Cells

AGS cells (5×10^5/well) were grown on glass coverslips (18-mm diameter; Fisher Scientific, Pittsburgh, PA). The culture media were exchanged fleshly 1 h before reagent treatment. The cells were incubated with various concentrations of H_2O_2 (0–0.5 mM) or with H_2O_2 (0.3 mM), eupatilin (200 μM), or H_2O_2 plus eupatilin for 1 h at 37°C. The cells were fixed for 15 min with 3.7% formaldehyde in PBS containing 0.1% Triton X-100 and 1 mM $MgCl_2$ (pH 7.2), stained with TRITC–phalloidin in PBS, and mounted with anti-fade solution (Molecular Probes). The slides were examined with an FV1000 confocal laser scanning microscope (Olympus corporation, Japan) equipped with ×40, ×60, and ×100 objectives and the data were analyzed by using the FLUOVIEW software ver.1.5 (Olympus corporation, Japan).

RNA Isolation

AGS cells ($1–3\times10^6$) were incubated for 1 h with eupatilin (200 μM), H_2O_2 (0.3 mM), or eupatilin plus H_2O_2, washed with serum-free media, and then further incubated at 37°C for the indicated time points in fresh media containing 10% FBS. Cells were harvested and total RNA was isolated using easy Blue (iNtRON Biotechnology, Korea) by the following manufacturer's instructions. The total RNA samples for quality were measured at 260/280 nm, 260/230 nm, and 28S/18S ratio.

cDNA Preparation and Microarray Hybridization

For each hybridization, dUTP-labeled cDNA was amplified from total RNA samples (5 μg per sample) by a RT-IVT Labeling Reagents (Applied Biosystems, MA). Approximately 50 μg labeled cDNA samples were subsequently purified by using a RT-IVT Purification Components (Applied Biosystems). The resulting samples were hybridized onto microarray chip containing oligonucleotide probes for 29,098 human genes (Applied Biosystems) and further processed according to the Applied Biosystems protocol.

Microarray Data Analysis

Microarray images and data were obtained and processed using the AB1700 microarray analyzer (Applied Biosystems) and Avadis Prophetic version 3.3 software (Strand Genomics, India). Briefly, the captured images were auto-gridded, and the signals were quantified and corrected for background. To select differentially expressed genes, the genes were filtered using Standard Expression Array System signal to noise threshold (S/N greater than 3 in at least three samples). The filtered genes were than normalized by the Lowess Regression normalization method. Genes with significantly different expression were identified using the t test ($P<0.05$) and the fold change method (Fold change>4). Fold changes were calculated from the average intensities of each replicated sample. Microarray experiment was repeated three times (three arrays per sample) to reduce a high risk of false-positive or false-negative results.

Semiquantitative RT-PCR

Semiquantitative RT-PCR was performed to validate the gene expression data resulted from microarray analysis. Each set of samples was analyzed in triplicate. The RNA samples used in RT-PCR experiments were identical to those used in microarray experiments. Reverse transcription of the RNA was performed using RT PreMix Kit (iNtRON Biotechnologyl). One microgram of RNA and 20 pmol primers were preincubated at 70°C for 5 min and transferred to a mixture tube. The reaction volume was 20 μl. cDNA synthesis was performed at 42°C for 60 min, followed by RT inactivation at 94°C for 5 min. Thereafter, the RT-generated DNA (2–5 μl) was amplified using PCR PreMix Kit (iNtRON Biotechnologyl). The primers used for cDNA amplification were: 5′-CAGAACATCCTGGAGCCTGTAAC-3′ (sense) and 5′-ATGTCCATTGCCTGATTCTTTGTG-3′ (antisense) for TNFRSF10A; 5′-CGGAGTCAACGGATTTGGTCGTAT-3′ (sense), 5′-AGCTTCTCCATGGTGGTGAAGAC-3′ (antisense) for HMOX 1; 5′-CATGCAGTGTAAGACCAA CGGGGA-3′ (sense), 5′-AATAGGTGACAGCCCGGCCA GAGT -3′ (antisense) for PLAUR; 5′-ATGACTTCCAAGC TGGCCGTGGCT-3′ (sense) and 5′-TCTCAGCCCTCTTC AAAAACTTCTC-3′ (antisense) for GDF 15; 5′-ATGTGCT GTACCAAGAGTTTG-3′ (sense) and 5′-TTACATGTTC TTGACTTTTTTACTGAGGAG-3′ (antisense) for ATF 3; 5′-CGGAGTCAACGGATTTGGTCGTAT-3′ (sense), 5′-AGCTTCTCCATGGTGGTGAAGAC-3′ (antisense) for GAPDH. Amplification conditions were denaturation at 94°C for 30 s, annealing at 56~65°C for 30 s, and extension at 72°C for 30 s for 30 cycles. The expected PCR products were 299 bp (for TNFRSF10A), 265 bp (for HMOX 1), 245 bp (for PLAUR), 120 bp (for GDF 15), 540 bp (for ATF 3), and 306 bp (for GAPDH). PCR products were subjected to electrophoresis on 1.2% agarose gel and were stained with ethidium bromide.

Real-Time Quantitative PCR

Real-time RT-PCR was performed to quantify the expression levels of TNFRSF10A, HMOX 1 and PLAUR, GDF15, ATF3 mRNA. The mRNA levels of cytokines were analyzed by quantitative real-time RT-PCR using DNA Engine with Chromo-4 Detector (MJ research, Waltham, MA). Total RNAs isolated using easy Blue (iNtRON Biotechnology, Korea) was reverse transcribed to cDNA using RT PreMix Kit (iNtRON Biotechnologyl). Obtained cDNA was subjected to quantitative real-time PCR in accordance with the manufacturer's instructions. PCR was performed in triplicates using 12.5 μl of SYBR Premix Ex Taq (Takara, Japan) and 2 μl of cDNA as a template in a 25 μl of final volume. PCR amplification was preceded by incubation of the mixture for 15 min at 95°C and 40 cycles of the amplification step consisted of denaturation, annealing and extension. The denaturation was performed for 30 s at 95°C, annealing was done in a transitional temperature range from 58°C to 62°C with a step-size of 0.5°C per cycle, and the extension was performed 30 s at 72°C with fluorescence detection after each cycle. After the final cycle, melting-point analyses of all samples were performed within the range from 65°C to 95°C with continuous fluorescence detection. Expression level of GAPDH was used for normalization.

Statistics

The mean values were calculated from data taken from at least three (usually four or more) separate experiments conducted on separate days. Microarray results were analyzed by the Student's *t* test. Other results in the text were analyzed by the ANOVA with post hoc test, where appropriate, by the Dunnett's test, using a commercial statistical software package (Instat®). A *P* value less than 0.05 was considered to indicate statistical significance.

RESULTS

Eupatilin Prevents the Delay of Wound Repair in AGS Cells Induced by H_2O_2

To evaluate the protective effect of eupatilin against oxidative stress, we initially tested whether eupatilin prevents the delay of wound repair in H_2O_2-treated cells. Representative wound assays are shown in Fig. 2A. The number of migrated cells into the wounded area was significantly delayed by treatment with H_2O_2 (Fig. 2A and B), as compared to that with no reagent (control). The results of a dose-dependent experiment revealed that the optimal inhibition was obtained with the 0.3 mM of H_2O_2 (**$p<0.001$; Fig. 2B). Eupatilin alone had no significant effect, whereas H_2O_2-induced delay of wound repair was significantly prevented by the treatment with eupatilin in a dose-dependent manner (100–500 μM; Fig. 2C). As shown in Fig. 3A, eupatilin could prevent the H_2O_2-induced inhibition of cell proliferation. However, this was not likely due to the effect of eupatilin-induced cell proliferation, because eupatilin by itself decreased the proliferation of AGS cells (Fig. 3B). We therefore performed cell viability assay to test whether the preventive effect of eupatilin on H_2O_2-induced inhibition of cell proliferation arises from its potential to protect cells from H_2O_2-induced cell death. As shown in Fig. 3C, treatment with eupatilin dramatically decreased H_2O_2-induced cell death, suggesting that the preventive effect of eupatilin against H_2O_2–induced delayed wound closure is due to the its ability to protect cells from oxidative stress.

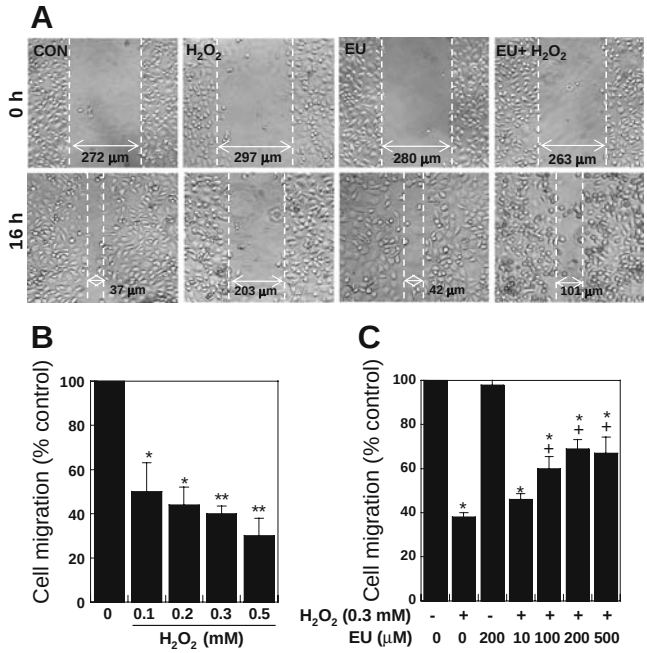

Fig. 2. Eupatilin prevents the delay of wound repair in AGS cells induced by H_2O_2. Confluent AGS cell monolayers in 12 well plates were wounded by introducing a linear scratch of ±0.3 mm width using a sterile pipette tip. Cells were pretreated for 1 h with H_2O_2 (0.1–0.5 mM), eupatilin (10–500 μM), or H_2O_2 plus eupatilin, washed with serum-free media, and then further incubated at 37°C for 16 h in fresh media containing 10% FBS. The extent of wound closure was monitored and quantitated by the analysis of the remaining wound areas using Olympus FLUOVIEW software. **A** Bright field images of the wound areas taken at 0 and 16 h, after incubation with the H_2O_2 (0.3 mM), eupatilin (200 μM), or H_2O_2 plus eupatilin. *EU* Eupatilin. The data were compared with the values obtained without H_2O_2 as control by ANOVA and Dunnett's test (*$P<0.05$, **$P<0.01$). **B** and **C** Quantitative analysis of the percentage of wound closure after 16 h of wound injury in AGS cell monolayers in the absence or presence of agents as indicated. ANOVA and post hoc Dunnett's test (*$P<0.05$ *vs* control ($-H_2O_2/-$EU); $^{+}P<0.05$ *vs* $+H_2O_2$). The *bar graphs* summarize the results from three to six independent experiments.

Eupatilin Prevents the H_2O_2-Induced Actin Disruption

It is now established that ROS can injure the mucosa by disruption of the cytoskeletal network, a key component of mucosal barrier integrity (19). We therefore investigated whether eupatilin prevents the instability of cytoskeletal protein actin. As shown in Fig. 4A, treatment of AGS cells with H_2O_2 (0.3 mM, 1 h) significantly disrupted the F-actin cytoskeleton, as determined by the actin staining with the TRITC-phalloidin and then high-resolution laser confocal microscopy. In contrast, pretreatment with eupatilin (200 μM) protected the F-actin cytoskeleton against oxidant damage as shown by the appearance of an intact and continuous pattern of actin at the site of plasma membrane (areas of cell-cell contact; Fig. 4B). As eupatilin has a preventive effect against H_2O_2–induced delayed wound closure, we further examined the F-actin cytoskeleton at 16 h after wound repair experiments, and observed that the cells which are migrated to the wounded area in H_2O_2 plus eupatilin-treated group reveal more intact F-actin cytoskeleton than that in H_2O_2-treated group (Fig. 4C).

Eupatilin Inhibits ROS Production

Based on the results obtained above, we hypothesized that the effects of eupatilin to protect AGS cells against oxidant damage are associated with its efficacy to scavenge ROS generated within the cells or derived from a variety of external sources. We therefore further examined whether eupatilin inhibits ROS generation in AGS cells stimulated by $FeSO_4$ [150 μM (18)]. As shown in Fig. 5A and B, treatment with eupatilin dramatically inhibited $FeSO_4$-induced ROS production in a dose-dependent manner and the inhibition levels were higher than that of achieved with anti-oxidant NAC at the same concentrations. Rebamipide, a novel quinolinone-derived gastroprotective agent used in Japan for the treatment of gastric ulcers, has been reported to provide gastroprotection through scavenging of free radicals (20). We therefore investigated the effects of rebamipide to scavenge $FeSO_4$-induced ROS production in AGS cells and compared them to that of eupatilin. As shown in Fig. 5A and

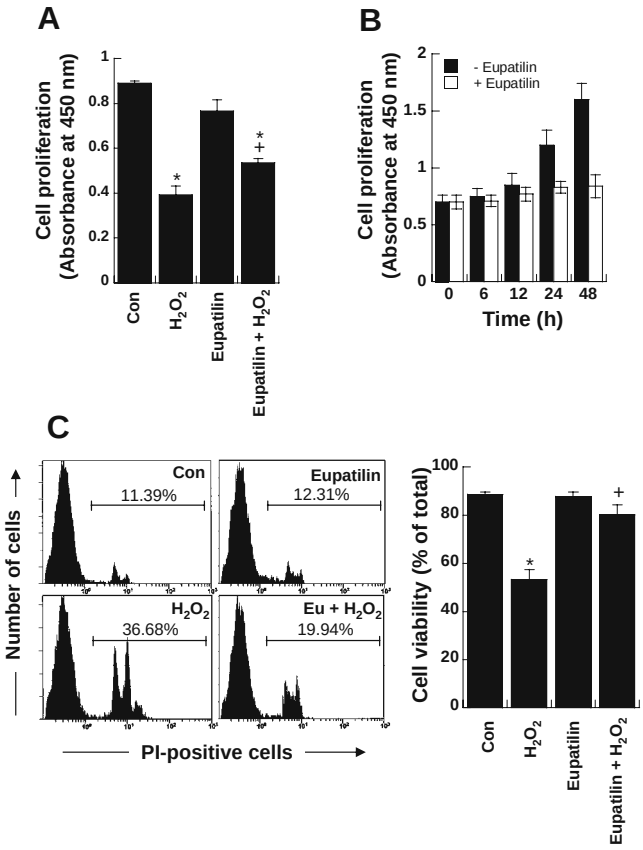

Fig. 3. Eupatilin rescues AGS cells from the H_2O_2-induced inhibition of cell proliferation. **A** Cells were pretreated for 1 h with H_2O_2 (0.3 mM), eupatilin (200 μM), or H_2O_2 plus eupatilin, washed with fresh media, and further incubated for 16 h in fresh media containing 10% FBS. Cell proliferation was determined as described in the *Materials and Methods* section. ANOVA and post hoc Dunnett's test (*$P<0.05$ *vs* control (vehicle treated); $^{+}P<0.05$ *vs* H_2O_2-treated cells). **B** Cells were treated with vehicle (0.1% DMSO) or eupatilin (200 μM), and further incubated for various time points (0–48 h). Cell proliferation was determined as above (**A**). **C** Cells from the above (**A**) were tested for cell viability as described in the *Materials and Methods* section. ANOVA and post hoc Dunnett's test (*$P<0.05$ vs control (PBS); $^{+}P<0.05$ *vs* H_2O_2-treated cells). The *bar graphs* summarize the results from three to six independent experiments.

C, the effect of rebamipide was less significant than that of eupatilin in terms of inhibition of $FeSO_4$-induced ROS production in AGS cells. The concentrations ranging from 10 to 500 μM of eupatilin showed no toxic effects at 16 h of incubation on AGS cells (Fig. 5D). Eupatilin also inhibited $FeSO_4$-induced ROS production in other cell types, e.g., J774 and human neutrophils (data not shown).

Although we demonstrated that eupatilin prevents H_2O_2-induced wound delay and actin disruption, these data do not allow a direct connection between the cellular effects and the effects on free radicals by eupatilin. We therefore further tested whether eupatilin also prevents $FeSO_4$-induced inhibition of cell proliferation as well as disruption of F-actin cytoskeleton. As shown in Fig. 6A, treatment with eupatilin significantly prevented the $FeSO_4$-induced inhibition of cell proliferation at the concentrations ranging from 10 to 500 μM of eupatilin. In addition, treatment of AGS cells with eupatilin protected the F-actin cytoskeleton against $FeSO_4$-induced damage (Fig. 6B).

Eupatilin Inhibits H_2O_2-Induced Heme Oxygenase-1 (HMOX-1) Expression in AGS Cells

In order to understand the protective role of eupatilin at the transcriptional level in H_2O_2-treated AGS cells, we analyzed the global gene expression patterns of AGS cells that were treated with H_2O_2 (0.3 mM). The expression profiles were surveyed through microarray experiments with

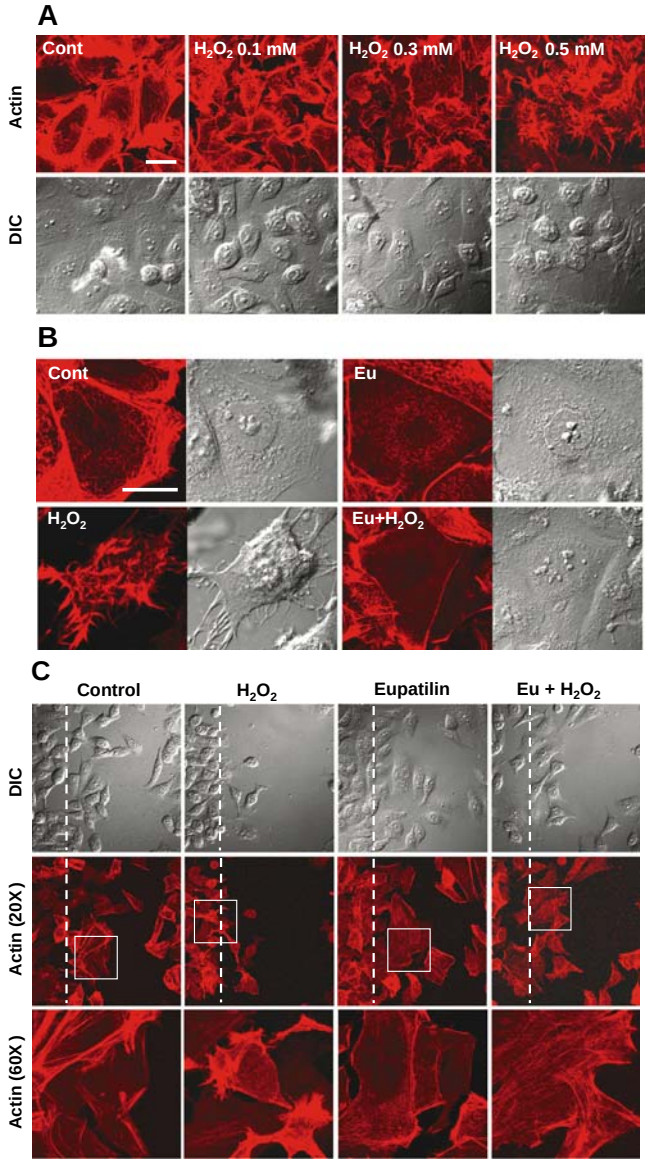

Fig. 4. Eupatilin inhibits H_2O_2-induced actin disruption in cultured AGS cells. **A** and **B** AGS cells (5×10^5/well) were grown on glass coverslips. The cells were incubated with various concentrations of H_2O_2 (0–0.5 mM; **A**) or with H_2O_2 (0.3 mM), eupatilin (200 μM), or H_2O_2 plus eupatilin (**B**) for 1 h at 37°C. The cells were fixed and stained with TRITC–phalloidin as described in the *Materials and Methods* section. The slides were examined with a FV1000 confocal laser scanning microscope (×40 or ×100), and the data were analyzed by using the FLUOVIEW software ver.1.5. *Bar*=10 μm. **C** Cells from Fig. 1A were also fixed and stained with TRITC–phalloidin. F-actin was observed as described in (**A**). The *white dashed line* indicates the boundary of initial wound (0 h). The results were similar in three independent experiments.

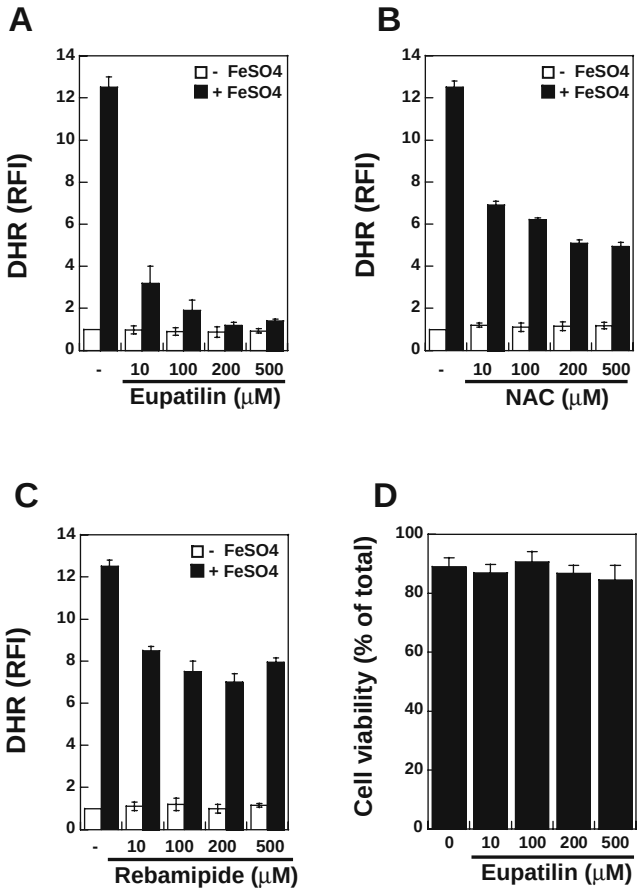

Fig. 5. Eupatilin inhibits $FeSO_4$-mediated ROS generation in cultured AGS cells. **A**–**C** AGS cells (5×10^5/well) were incubated with the various concentrations of eupatilin (10–500 μM; **A**), NAC (10–500 μM; **B**), or rebamipide (10–500 μM; **C**) in the presence or absence of $FeSO_4$ (150 μM). After 30 min, the fluorescent intensity for DHR was recorded using fluorescent plate reader at excitation of 507 nm and emission of 529 nm. The *bar graphs* summarize the results from three to five independent experiments. **D** AGS cells were treated with eupatilin (10–500 μM) for 16 h. Cell viability was determined by PI incorporation (mean ± SD, $n=3$).

oligonucleotide probes for 29,098 human genes. Student's *t*-test was used for determining significant changes in gene expression between untreated and H_2O_2-treated AGS cells. The expression levels of each gene from untreated *vs.* H_2O_2-treated AGS cells are presented as fold change, as compared with the control. 57 genes were found to be differentially expressed with a cutoff ($p<0.05$ and fold change>4). Among the 57 genes, 42 genes were up-regulated and some of up-regulated genes were involved in inflammation, oxidative stress, cell growth/proliferation, cellular protein metabolism and cytoskeleton organization. The known individual genes (>4-fold up-regulated by H_2O_2) are listed in Table 1. To validate the accuracy of microarray expression profiling data, we performed semi-quantitative RT-PCR and real-time quantitative PCR with several genes such as GDF15, ATF3, PLAUR, TNFRSF10A, and HMOX1 (HO-1), and confirmed that the three methods show overall qualitative agreement (Fig. 7). To further test whether eupatilin inhibits the expression of these potential candidate genes induced by oxidative stress (21–25), we performed the gene expression studies in the presence of H_2O_2, eupatilin, or H_2O_2 plus eupatilin. As shown in Fig. 8, eupatilin markedly reduced HO-1 expression, and weakly inhibited PLAUR and TNFRSF10A expression in H_2O_2-treated cells. Interestingly, however, other genes such as GDF15 and ATF3 were not down-modulated, but instead, they were induced by eupatilin and the induction was more significant in the presence of H_2O_2. This may explain the pro-apoptotic effects of eupatilin, as the expression of both GDF15 and ATF3 genes are known to be associated in p53-dependent pathways in various cells (26–28).

DISCUSSION

A loss of gastric mucosal barrier integrity has been implicated as one of the key mechanisms underlying the pathophysiology of oxidative inflammatory disorders in stomach (29,30). Accordingly, characterizing a therapeutically effective means of protecting gastric barrier function under conditions of oxidant-induced injury, as the present investi-

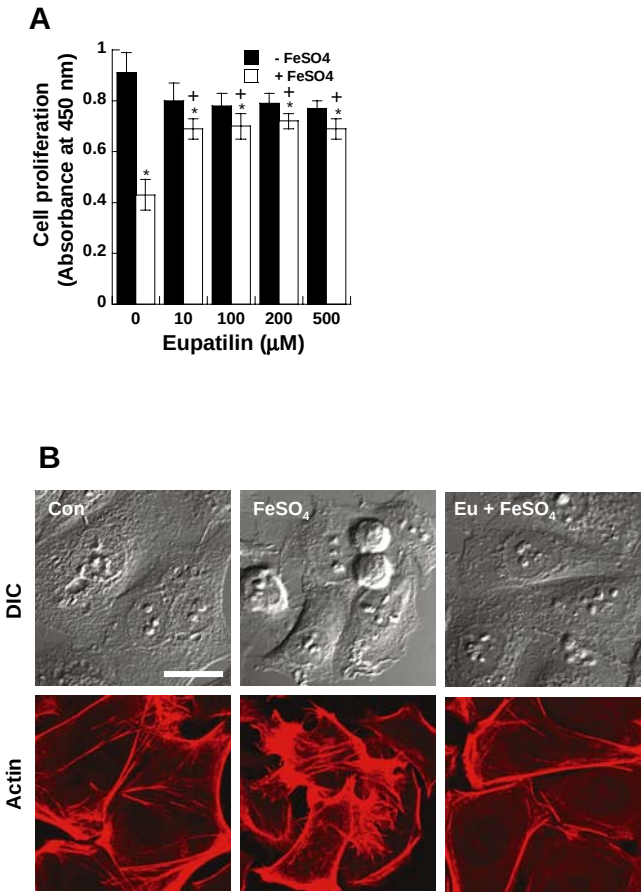

Fig. 6. Eupatilin prevents the $FeSO_4$-induced inhibition of cell proliferation and actin disruption in cultured AGS cells. **A** Cells were treated with $FeSO_4$ (150 μM), eupatilin (200 μM), or $FeSO_4$ plus eupatilin for 16 h in Ham's F12 medium containing 10% FBS. Cell proliferation was determined as described in the *Materials and Methods* section. ANOVA and post hoc Dunnett's test (*$P<0.05$ *vs* control ($-FeSO_4$); $^+P<0.05$ *vs* $FeSO_4$-treated cells). **B** AGS cells (5×10^5/well) were grown on glass coverslips. The cells were incubated for 1 h with $FeSO_4$ (150 μM) or $FeSO_4$ plus eupatilin (200 μM) at 37°C. F-actin was stained and examined as described above (Fig. 4). *Bar*=10 μm.

Table 1. Genes Whose Expression was 4-Fold Over-Induced in H_2O_2-Treated AGS Cells[a]

Gene_Name	Gene_Symbol	RefSeq_NM	Fold Change (H_2O_2/control)
Growth differentiation factor 15	GDF15	NM_002575	27.21
Activating transcription factor 3	ATF3	NM_002659	18.02
Early growth response 1	EGR1	NM_001964	8.29
Plasminogen activator, urokinase receptor	PLAUR	NM_001613	7.43
Pre-mRNA cleavage complex II protein Pcf11	PCF11	NM_001065	7.30
Tumor necrosis factor receptor superfamily, member 10a	TNFRSF10A	NM_003844	7.20
Serine (or cysteine) proteinase inhibitor, clade B (ovalbumin), member 2	SERPINB2	NM_014330	7.15
Phorbol-12-myristate-13-acetate-induced protein 1	PMAIP1	NM_021127	6.78
Protein phosphatase 1, regulatory (inhibitor) subunit 15A	PPP1R15A	NM_014330	6.56
Cyclin-dependent kinase inhibitor 1A (p21, Cip1)"	CDKN1A	NM_002133	6.50
Heme oxygenase (decycling) 1	HMOX1	NM_006622	6.14
Myosin IXA	MYO9A	NM_006901	5.71
NACHT, leucine rich repeat and PYD containing 1	NALP1	NM_000389	5.47
Actin, alpha 2, smooth muscle, aorta	ACTA2	NM_001613	5.36
Integrin, alpha 2 (CD49B, alpha 2 subunit of VLA-2 receptor)	ITGA2	NM_000341	5.29
Tumor necrosis factor receptor superfamily, member 10d, decoy with truncated death domain	TNFRSF10D	NM_003840	5.18
Ras homolog gene family, member E	ARHE	NM_006901	4.97
Mdm2, transformed 3T3 cell double minute 2, p53 binding protein (mouse)	MDM2	NM_001049	4.83
Polo-like kinase 2 (Drosophila)	PLK2	NM_003447	4.81
Growth arrest-specific 8	GAS8	NM_001481	4.70
EPH receptor A2	EPHA2	NM_004431	4.68
CMT1A duplicated region transcript 1	CDRT1	NM_006382	4.47
Sestrin 2	SESN2	NM_031459	4.35
Keratin associated protein 10–7	KRTAP10–7	NM_198689	4.30
Activating transcription factor 4 (tax-responsive enhancer element B67)	ATF4	NM_015885	4.28
Zinc finger, DHHC domain containing 11	ZDHHC11	NM_024786	4.19
Advillin	AVIL	NM_152362	4.17
Chloride channel 2	CLCN2	NM_022782	4.11
Leukemia inhibitory factor (cholinergic differentiation factor)	LIF	NM_021127	4.04
Tumor necrosis factor receptor superfamily, member 1A	TNFRSF1A	NM_005168	4.03

[a] AGS cells (3×10^6) were incubated for 1 h with H_2O_2 (0.3 mM), washed, and then further incubated for 3 h at 37°C in complete media. Total RNA was isolated and analyzed by DNA microarray hybridization.

gation has done, is of significant clinical importance with potentially important implication for the treatment of a variety of inflammatory disorders. In the present study, we demonstrated, for the first time, that eupatilin prevents the reduction of cell migration and disruption of actin cytoskeleton induced by H_2O_2. Eupatilin also inhibited $FeSO_4$-induced ROS generation in various cell types, including AGS cells, J774 cells and neutrophils. Moreover, eupatilin prevented $FeSO_4$-induced cell growth inhibition and F-actin disruption, thereby suggesting a strong relationship between cellular protective effect of eupatilin and its inhibitory effect on ROS production. In support of these findings, eupatilin dramatically reduced the expression of HO-1, an oxidative-stress responsible gene, by H_2O_2 in AGS cells. Thus, we demonstrate here a novel role for eupatilin in oxidant-induced injury rather than its better characterized effect as an apoptotic inducer in various cells.

A previous study using gastric epithelial cells showed that H_2O_2 inhibited cell migration and proliferation, probably by inhibiting the formation and ruffling movement of lamellipodia or by disrupting the actin cytoskeleton (19,31). In the present study, H_2O_2 significantly suppressed the migration of AGS cells into wounded areas. We found that the preventive effect of eupatilin in H_2O_2-induced suppression of cell migration was not related to the cellular proliferation, as eupatilin had no promoting effect on cell proliferation. Instead, we suggest that attenuation of actin disruption is critical for the action of eupatilin in preventing the delayed migration in H_2O_2-treated AGS cells. Indeed, we now understand that actin dynamics is critical for epithelial cell migration (32).

Given the importance of gastrointestinal barrier function in the body homeostasis, it may be essential to develop agents that have a potential to protect barrier function under conditions of oxidant-induced injury. In this sense, a good example is rebamipide, a novel quinolinone-derived gastroprotective agent used in Japan for the treatment of gastritis and gastric ulcers (33). Previous reports demonstrated that rebamipide is an effective cytoprotective agent against oxidant-induced actin cytoskeletal instability and cellular apoptosis (19,31). These results also suggested that the cytoprotective effects of rebamipide are possibly through the radical scavenging action (19,31). In a good agreement with this line, our present results also demonstrated that eupatilin dramatically

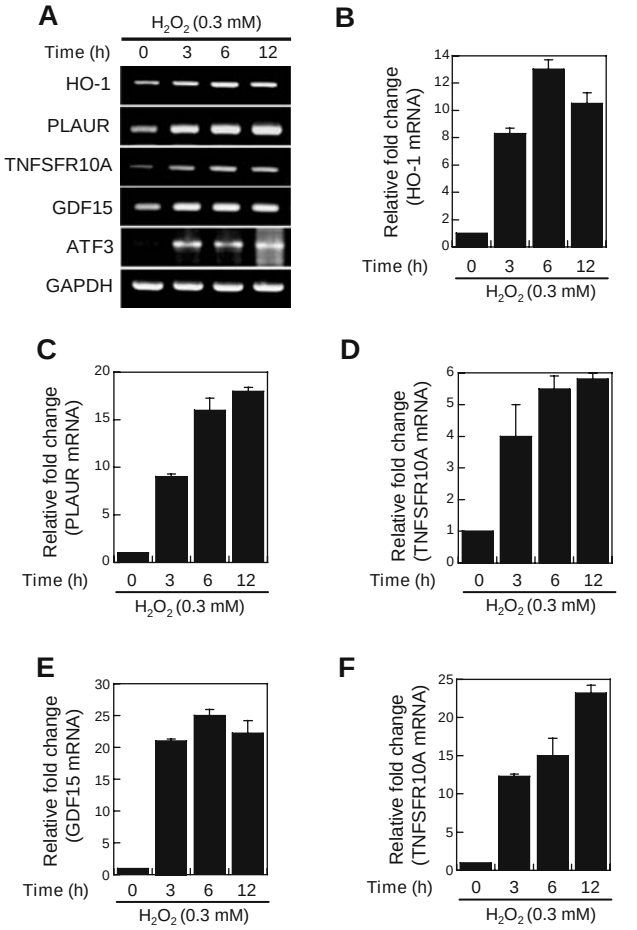

Fig. 7. Validation of H_2O_2-responsible genes by semi-quantitative RT-PCR and real-time PCR. AGS cells (1×10^6/well) were pretreated for 1 h with H_2O_2 (0.3 mM), washed, and further incubated in complete medium for the indicated time points (0–12 h). Levels of mRNA were determined by semiquantitative RT-PCR (**A**) and real-time PCR (**B**–**F**), as described in the *Materials and Methods* section. The results were similar in three independent experiments.

inhibits $FeSO_4$-induced ROS production in such cells as AGS, J774 cells, and neutrophils. More directly, eupatilin significantly attenuated F-actin disruption by $FeSO_4$ in AGS cells.

Genetic chip technology is characterized by high communication, low consumption and miniaturization (34,35), providing a technological platform to study the mechanism of herbal medicines against various biological disorders including oxidative stress-related diseases. To gain molecular insight into the biological mechanisms played by eupatilin in H_2O_2-induced cell damage, we first investigated the gene expression patterns in H_2O_2-treated cells using microarray technology. We identified a variety of genes with altered expression in H_2O_2-treated cells, including genes for inflammation, oxidative stress, cell growth/proliferation, cellular protein metabolism and cytoskeleton organization (Table 1). Among those H_2O_2-responsible genes, selective inhibition of H_2O_2-induced expression of HO-1 by eupatilin further suggests a novel role for eupatilin in oxidant-induced injury. However, it was interesting to be noticed that such genes as GDF15 and ATF3 are not down-modulated, but instead, they were induced by eupatilin and the induction was more significant in the presence of H_2O_2. This result may suggest that eupatilin has dual functions, i.e., cytoprotective effect against oxidant-induced injury and pro-apoptotic function in some cell types. Previous report demonstrated that eupatilin-induced apoptotic cell death is associated with the elevated expression of p53 and p21 (6). Indeed, the expression of both GDF15 and ATF3 genes are known to be associated in p53-dependent pathways in various cells (26–28). Meanwhile, it is also possible that transcription factors involved in the H_2O_2-mediated induction of these two genes are different from that of the HO-1 gene. For example, HO-1 induction is known to be regulated by the transcription factors AP-1, AP-2, NF-κB, and Nrf-2 in various cellular systems (36–38). Although ATF3 has similar binding sites as seen in HO-1 promoter, other sites such as ATF/CRE, E2F and Myc/Max are also reported (39).

Cell-based experiment is valuable not only for rapid screening of potential therapeutic agents but also for gaining

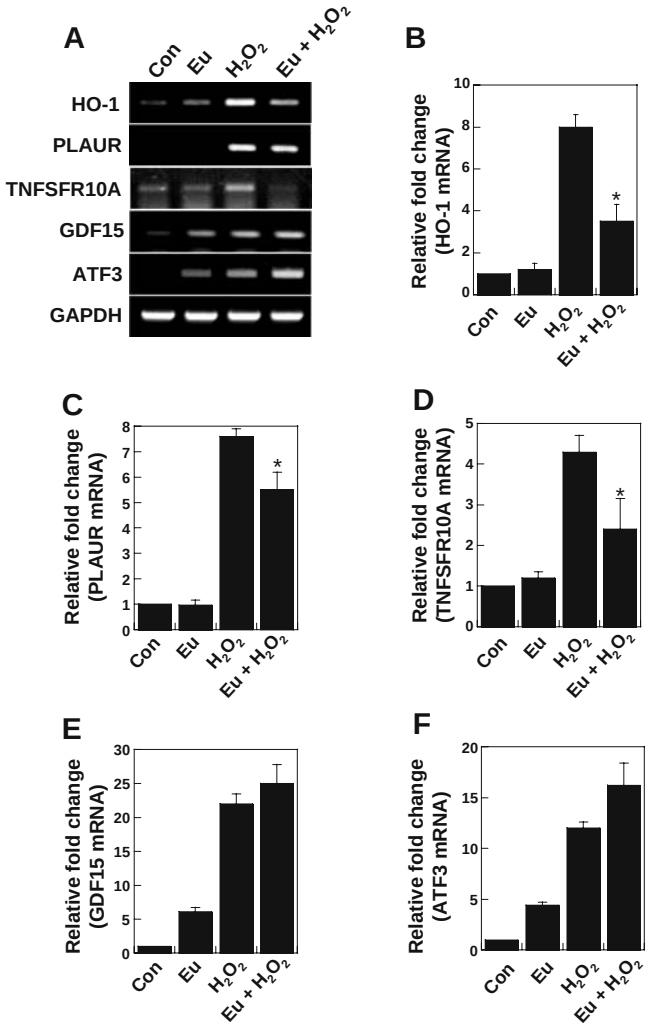

Fig. 8. Inhibition of H_2O_2-responsible genes by eupatilin. AGS cells (1×10^6/well) were pretreated for 1 h with H_2O_2 (0.3 mM), eupatilin (200 μM), or H_2O_2 plus eupatilin, washed, and further incubated in complete medium for 3 h. Levels of mRNA were determined by semiquantitative RT-PCR (**A**) and real-time PCR (**B**–**F**), as described in the *Materials and Methods* section. The results were similar in three to five independent experiments. ANOVA and post hoc Dunnett's test (*$P<0.05$ *vs* H_2O_2-treated cells).

mechanistic insights not accessible otherwise. However, the observations made in cultured cells need to be confirmed using appropriate animal models to test *in vivo* significance of the cellular findings. Moreover, *in vivo* efficacy testing of potential therapeutic agents is a prerequisite for their further development as clinically useful agents. It has been demonstrated that oral administration of DA-9601 at 40 mg/kg body weight was known to reduce ethanol-induced gastric mucosal hemorrhagic lesions and lipid peroxidation (4). Indeed, this concentration contains approximately 0.7 mg/kg of eupatilin, which is equal to the concentration of the 40 μM eupatilin in 1 ml PBS/mouse. Therefore, the present study strongly suggests an *in vivo* relevance of eupatilin effect in terms of its anti-oxidative property.

Taken together, our current results describing the protective effect of eupatilin against oxidative damage will contribute to the elucidation of the efficacy of eupatilin in protecting gastric mucosal ulceration. Further, these results indicate a potential mechanism in the therapeutic activity of DA-9601 (Stillen™) in the treatment of diseases characterized by gastric mucosal ulceration.

ACKNOWLEDGEMENT

This work was supported by the Korea Research Foundation Grant (R05-2004-000-11388-0) and the Korea Health 21 R&D Project, Ministry of Health & Welfare (01-PJ3-PG6-01GN09-003).

REFERENCES

1. K. B. Hahm, J. H. Kim, B. M. You, Y. S. Kim, S. W. Cho, H. Yim, B. O. Ahn, and W. B. Kim. Induction of apoptosis with an extract of Artemisia asiatica attenuates the severity of cerulein-induced pancreatitis in rats. *Pancreas* **17**:153–157 (1998).
2. B. K. Ryu, B. O. Ahn, T. Y. Oh, S. H. Kim, W. B. Kim, and E. B. Lee. Studies on protective effect of DA-9601, Artemisia asiatica extract, on acetaminophen- and CCl4-induced liver damage in rats. *Arch. Pharm. Res.* **21**:508–513 (1998).
3. T. Y. Oh, J. S. Lee, B. O. Ahn, H. Cho, W. B. Kim, Y. B. Kim, Y. J. Surh, S. W. Cho, K. M. Lee, and K. B. Hahm. Oxidative stress is more important than acid in the pathogenesis of reflux oesophagitis in rats. *Gut* **49**:364–371 (2001).
4. K. Huh, T. H. Kwon, U. S. Shin, W. B. Kim, B. O. Ahn, T. Y. Oh, and J. A. Kim. Inhibitory effects of DA-9601 on ethanol-induced gastrohemorrhagic lesions and gastric xanthine oxidase activity in rats. *J. Ethnopharmacol.* **88**:269–273 (2003).
5. H. J. Seo, and Y. J. Surh. Eupatilin, a pharmacologically active flavone derived from Artemisia plants, induces apoptosis in human promyelocytic leukemia cells. *Mutat. Res.* **496**:191–198 (2001).
6. M. J. Kim, D. H. Kim, H. K. Na, T. Y. Oh, C. Y. Shin, and D. P. Y. J. Surh Ph. Eupatilin, a pharmacologically active flavone derived from Artemisia plants, induces apoptosis in human gastric cancer (AGS) cells. *J. Environ. Pathol. Toxicol. Oncol.* **24**:261–269 (2005).
7. D. H. Kim, H. K. Na, T. Y. Oh, C. Y. Shin, and Y. J. Surh. Eupatilin inhibits proliferation of ras-transformed human breast epithelial (MCF-10A-ras) cells. *J. Environ. Pathol. Toxicol. Oncol.* **24**:251–259 (2005).
8. D. H. Kim, H. K. Na, T. Y. Oh, W. B. Kim, and Y. J. Surh. Eupatilin, a pharmacologically active flavone derived from Artemisia plants, induces cell cycle arrest in ras-transformed human mammary epithelial cells. *Biochem. Pharmacol.* **68**:1081–1087 (2004).
9. W. Ren, Z. Qiao, H. Wang, L. Zhu, and L. Zhang. Flavonoids: promising anticancer agents. *Med. Res. Rev.* **23**:519–534 (2003).
10. Z. Horvath, S. Marihart-Fazekas, P. Saiko, M. Grusch, M. Ozsuy, M. Harik, N. Handler, T. Erker, W. Jaeger, M. Fritzer-Szekeres, B. Djavan, and T. Szekeres. Novel resveratrol derivatives induce apoptosis and cause cell cycle arrest in prostate cancer cell lines. *Anticancer Res.* **27**:3459–3464 (2007).
11. J. W. Park, K. J. Woo, J. T. Lee, J. H. Lim, T. J. Lee, S. H. Kim, Y. H. Choi, and T. K. Kwon. Resveratrol induces pro-apoptotic endoplasmic reticulum stress in human colon cancer cells. *Oncol. Rep.* **18**:1269–1273 (2007).
12. V. Cecchinato, R. Chiaramonte, M. Nizzardo, B. Cristofaro, A. Basile, G. V. Sherbet, and P. Comi. Resveratrol-induced apoptosis in human T-cell acute lymphoblastic leukaemia MOLT-4 cells. *Biochem. Pharmacol.* **74**:1568–1574 (2007).
13. Q. H. Gong, Q. Wang, J. S. Shi, X. N. Huang, Q. Liu, and H. Ma. Inhibition of caspases and intracellular free Ca2+ concentrations are involved in resveratrol protection against apoptosis in rat primary neuron cultures. *Acta Pharmacol. Sin.* **28**:1724–1730 (2007).
14. T. West, M. Atzeva, and D. M. Holtzman. Pomegranate polyphenols and resveratrol protect the neonatal brain against hypoxic–ischemic injury. *Dev. Neurosci.* **29**:363–372 (2007).
15. M. K. Lee, S. J. Kang, M. Poncz, K. J. Song, and K. S. Park. Resveratrol protects SH-SY5Y neuroblastoma cells from apoptosis induced by dopamine. *Exp. Mol. Med.* **39**:376–384 (2007).
16. I. Rahman, and I. Kilty. Antioxidant therapeutic targets in COPD. *Current Drug Targets* **7**:707–720 (2006).
17. M. Ishiyama, H. Tominaga, M. Shiga, K. Sasamoto, Y. Ohkura, and K. Ueno. A combined assay of cell viability and *in vitro* cytotoxicity with a highly water-soluble tetrazolium salt, neutral red and crystal violet. *Biol. Pharm. Bull.* **19**:1518–1520 (1996).
18. J. A. Royalland, and H. Ischiropoulos. Evaluation of 2′,7′-dichlorofluorescin and dihydrorhodamine 123 as fluorescent probes for intracellular H2O2 in cultured endothelial cells. *Arch. Biochem. Biophys.* **302**:348–355 (1993).
19. A. Banan, L. Fitzpatrick, Y. Zhang, and A. Keshavarzian. OPC-compounds prevent oxidant-induced carbonylation and depolymerization of the F-actin cytoskeleton and intestinal barrier hyperpermeability. *Free Radic. Biol. Med.* **30**:287–298 (2001).
20. S. Iinuma, Y. Naito, T. Yoshikawa, S. Takahashi, T. Takemura, N. Yoshida, and M. Kondo. *In vitro* studies indicating antioxidative properties of rebamipide. *Dig. Dis. Sci.* **43**:35S–39S (1998).
21. D. Schlittenhardt, A. Schober, J. Strelau, G. A. Bonaterra, W. Schmiedt, K. Unsicker, J. Metz, and R. Kinscherf. Involvement of growth differentiation factor-15/macrophage inhibitory cytokine-1 (GDF-15/MIC-1) in oxLDL-induced apoptosis of human macrophages *in vitro* and in arteriosclerotic lesions. *Cell Tissue Res.* **318**:325–333 (2004).
22. J. Kool, M. Hamdi, P. Cornelissen-Steijger, A. J. van der Eb, C. Terleth, and H. van Dam. Induction of ATF3 by ionizing radiation is mediated via a signaling pathway that includes ATM, Nibrin1, stress-induced MAPkinases and ATF-2. *Oncogene* **22**:4235–4242 (2003).
23. K. Z. Guyton, D. R. Spitz, and N. J. Holbrook. Expression of stress response genes GADD153, c-jun, and heme oxygenase-1 in H2O2- and O2-resistant fibroblasts. *Free Radic Biol. Med.* **20**:735–741 (1996).
24. H. Oka, K. Kugiyama, H. Doi, T. Matsumura, H. Shibata, L. A. Miles, S. Sugiyama, and H. Yasue. Lysophosphatidylcholine induces urokinase-type plasminogen activator and its receptor in human macrophages partly through redox-sensitive pathway. *Arterioscler. Thromb. Vasc. Biol.* **20**:244–250 (2000).
25. A. M. Choi, and J. Alam. Heme oxygenase-1: function, regulation, and implication of a novel stress-inducible protein in oxidant-induced lung injury. *Am. J. Respir. Cell Mol. Biol.* **15**:9–19 (1996).
26. G. Yang, G. Zhang, M. R. Pittelkow, M. Ramoni, and H. Tsao. Expression Profiling of UVB Response in Melanocytes Identifies a Set of p53-Target Genes. *J. Invest. Dermatol.* **126**:2490–2506 (2006).
27. K. Kannan, N. Amariglio, G. Rechavi, J. Jakob-Hirsch, I. Kela, N. Kaminski, G. Getz, E. Domany, and D. Givol. DNA microarrays identification of primary and secondary target genes regulated by p53. *Oncogene* **20**:2225–2234 (2001).

28. P. Secchiero, E. Barbarotto, M. Tiribelli, C. Zerbinati, M. G. di Iasio, A. Gonelli, F. Cavazzini, D. Campioni, R. Fanin, A. Cuneo, and G. Zauli. Functional integrity of the p53-mediated apoptotic pathway induced by the nongenotoxic agent nutlin-3 in B-cell chronic lymphocytic leukemia (B-CLL). *Blood* **107**:4122–4129 (2006).
29. T. Yoshikawa, and Y. Naito. The role of neutrophils and inflammation in gastric mucosal injury. *Free Radic. Res.* **33**:785–794 (2000).
30. G. M. Matthews, and R. N. Butler. Cellular mucosal defense during Helicobacter pylori infection: a review of the role of glutathione and the oxidative pentose pathway. *Helicobacter* **10**:298–306 (2005).
31. S. Watanabe, X. E. Wang, M. Hirose, T. Osada, H. Tanaka, and N. Sato. Rebamipide prevented delay of wound repair induced by hydrogen peroxide and suppressed apoptosis of gastric epithelial cells *in vitro*. *Dig. Dis. Sci.* **43**:107S–112S (1998).
32. P. Friedl. Prespecification and plasticity: shifting mechanisms of cell migration. *Curr. Opin. Cell Biol.* **16**:14–23 (2004).
33. K. Yamasaki, T. Kanbe, T. Chijiwa, H. Ishiyama, and S. Morita. Gastric mucosal protection by OPC-12759, a novel antiulcer compound, in the rat. *Eur. J. Pharmacol.* **142**:23–29 (1987).
34. R. Vittal, Z. E. Selvanayagam, Y. Sun, J. Hong, F. Liu, K. V. Chin, and C. S. Yang. Gene expression changes induced by green tea polyphenol (−)-epigallocatechin-3-gallate in human bronchial epithelial 21BES cells analyzed by DNA microarray. *Mol. Cancer Ther.* **3**:1091–1099 (2004).
35. Y. Takahashi, J. A. Lavigne, S. D. Hursting, G. V. Chandramouli, S. N. Perkins, J. C. Barrett, and T. T. Wang. Using DNA microarray analyses to elucidate the effects of genistein in androgen-responsive prostate cancer cells: identification of novel targets. *Mol. Carcinog.* **41**:108–119 (2004).
36. J. Alam, and Z. Den. Distal AP-1 binding sites mediate basal level enhancement and TPA induction of the mouse heme oxygenase-1 gene. *J. Biol. Chem.* **267**:21894–21900 (1992).
37. Y. Lavrovsky, M. L. Schwartzman, R. D. Levere, A. Kappas, and N. G. Abraham. Identification of binding sites for transcription factors NF-kappa B and AP-2 in the promoter region of the human heme oxygenase 1 gene. *Proc. Natl. Acad. Sci. USA* **91**:5987–5991 (1994).
38. C. H. He, P. Gong, B. Hu, D. Stewart, M. E. Choi, A. M. Choi, and J. Alam. Identification of activating transcription factor 4 (ATF4) as an Nrf2-interacting protein. Implication for heme oxygenase-1 gene regulation. *J. Biol. Chem.* **276**:20858–20865 (2001).
39. G. Liang, C. D. Wolfgang, B. P. Chen, T. H. Chen, and T. Hai. ATF3 gene. Genomic organization, promoter, and regulation. *J. Biol. Chem.* **271**:1695–1701 (1996).